

Supporting Information; Simulation of Defect Reduction in Block Copolymer Thin Films by Solvent Annealing

Su-Mi Hur,^{†,‡} Gurdaman S. Khaira,[†] Abelardo Ramírez-Hernández,^{†,‡} Marcus Müller,[¶] Paul F. Nealey,^{†,§} and Juan J. de Pablo^{*,†,§}

Materials Science Division, Argonne National Laboratory, 9700 South Cass Avenue, Argonne, Illinois 60439, United States, Institute for Molecular Engineering, The University of Chicago, Chicago, Illinois 60637, USA, Institut für Theoretische Physik, Georg-August-Universität, 37077 Göttingen, Germany, and Institute for Molecular Engineering, The University of Chicago, Chicago, Illinois 60637, United States

E-mail: depablo@uchicago.edu

Model Description

To model solvent-assisted block copolymer self-assembly, we rely on a Theoretically Informed Coarse Grained (TICG) simulation method, which has been successfully applied to study the phase behavior of block copolymer thin films. Polymers are represented by discretized Gaussian chains composed by N beads. At temperature T , the bonded energy associated to

^{*}To whom correspondence should be addressed

[†]Materials Science Division, Argonne National Laboratory, 9700 South Cass Avenue, Argonne, Illinois 60439, United States

[‡]Institute for Molecular Engineering, The University of Chicago, Chicago, Illinois 60637, USA

[¶]Institut für Theoretische Physik, Georg-August-Universität, 37077 Göttingen, Germany

[§]Institute for Molecular Engineering, The University of Chicago, Chicago, Illinois 60637, United States

n chains is given by

$$\frac{H_b}{k_B T} = \frac{3}{2} \frac{N-1}{R_e^2} \sum_{k=1}^n \sum_{i=1}^{N-1} \mathbf{b}_k^2(i), \quad (1)$$

where $\mathbf{b}_k(i)$ is bond vector of the bond i in the k^{th} chain, k_B is Boltzmann's constant and R_e is the end-to-end distance for an ideal chain. We adopt a non-bonded interaction Hamiltonian through functional expansion in terms of number densities up to third order, according to

$$\frac{H_{nb}}{k_B T} = \int_V d\mathbf{x} \left\{ \frac{1}{2} \sum_{\alpha, \beta} \nu_{\alpha\beta} \frac{\rho_\alpha}{N} \frac{\rho_\beta}{N} + \frac{1}{3} \sum_{\alpha, \beta, \gamma} \omega_{\alpha\beta\gamma} \frac{\rho_\alpha}{N} \frac{\rho_\beta}{N} \frac{\rho_\gamma}{N} \right\} \quad (2)$$

where ρ_α is the number density of species α per unit volume, R_e^3 . This allows us to predict phenomena occurring at the interface between the polymer film and the solvent vapor. $\nu_{\alpha\beta}$ and $\omega_{\alpha\beta\gamma}$ are second and third-order virial coefficients. The indices α , β and γ run over the segment species A, B and solvent. This type of energy functional has been used to predict the phase behavior of mixed polymer brushes,¹ and it has been applied to various problems including the stability of polymer solution droplets and solvent evaporation from free standing polymer solutions.² Our approach considers three classes of interactions between polymer-polymer, solvent-solvent and polymer-solvent molecules. We choose virial coefficients for polymer-polymer interactions ν_{pp} and ω_{ppp} such that the vapor pressure of polymer molecules is negligible, and that the polymer has a finite coarse-grained compressibility;³

$$\nu_{pp} = -2 \frac{\kappa N + 3}{\sqrt{N}} \quad \text{and} \quad \omega_{ppp} = \frac{3}{2} \frac{\kappa N + 2}{\sqrt{N}^2}. \quad (3)$$

As shown by the sign of each parameter, ν_{pp} leads to an attraction between particles, while the third-order term ω_{ppp} is dominated by repulsions. Solvent-solvent interaction parameters, ν_{ss} and ω_{sss} , are determined by fitting the equation of state for the solvent. Fitting the isotherm for acetone at 300K gives values of $\nu_{ss} = -0.1399$; and $\omega_{sss} = 3.0246 \cdot 10^{-5}$. Cross-interaction coefficients between different polymer species A and B in the block copolymer

(ν_{AB} , ω_{AAB} and ω_{ABB}) and between polymer and solvent (ν_{ps} , ω_{pps} and ω_{pss}) are estimated by equating enthalpic terms of $\frac{\partial\mu}{\partial\phi}$ with that of the Flory-Huggins model, where μ is the mean-field exchange chemical potential of the homogeneous mixed system, which represents the change in free energy of the solution when N solvent particles are replaced by a polymer chain. For simplicity, we have also assumed isometric mixing. The enthalpic part in $\frac{\partial\mu}{\partial\phi}$ for the Flory-Huggins model is $-2\chi_{\alpha\beta}N$, while for our model it is $\sqrt{N}[\nu_{\alpha\alpha} + \nu_{\beta\beta} - 2\nu_{\alpha\beta}] + \sqrt{N}^2[2\omega_{\alpha\alpha\alpha}\phi_\alpha + 2\omega_{\alpha\alpha\beta} - 6\omega_{\alpha\alpha\beta}\phi_\alpha - 4\omega_{\alpha\beta\beta} + 6\omega_{\alpha\beta\beta}\phi_\alpha + 2\omega_{\beta\beta\beta} - 2\omega_{\beta\beta\beta}\phi_\alpha]$. If we choose cross terms as an arithmetic mean of $\omega_{\alpha\alpha\alpha}$ and $\omega_{\beta\beta\beta}$, such as, $\omega_{\alpha\alpha\beta} = \frac{2\omega_{\alpha\alpha\alpha} + \omega_{\beta\beta\beta}}{3}$ the third-order term in $\frac{\partial\mu}{\partial\phi}$ cancels out. We are then left with only the second-order term, which can be chosen to be compatible with the Flory-Huggins model

$$\nu_{\alpha\beta} = \chi N / \sqrt{N} + \frac{\nu_{\alpha\alpha} + \nu_{\beta\beta}}{2}. \quad (4)$$

Since the volumes of the coarse-grained polymer beads and solvent particles are modeled differently, interaction coefficients are modified with an asymmetric factor of the form

$$\nu_{ps} = \chi N / \sqrt{N} + \frac{1}{2} \left[\frac{\nu_{ps}}{C_s} + \nu_{ss} C_s \right] \quad (5)$$

where C_s is the volume ratio between polymer beads and solvent particles.

Table S1: Explicit numerical values of the virial coefficients that have used for $\sqrt{N} = 112$, $\kappa N = 100$, $\chi_{AB}N = 100$ and $C_s=30$.

$\nu_{AA} = \nu_{BB}$	-1.8393	$\omega_{AAA} = \omega_{BBB}$	0.012197	ν_{AB}	-0.94643
$\omega_{ABB} = \omega_{AAB}$	0.012197	ν_{ss}	-0.1399	ν_{sss}	$3.0246 \cdot 10^{-5}$
$\nu_{As} = \nu_{Bs}$	-2.1292	$\omega_{Ass} = \omega_{Bss}$	$6.0944 \cdot 10^{-4}$	$\omega_{AAs} = \omega_{BBs}$	$9.3448 \cdot 10^{-3}$

Deviations from the simple dilution approximation, namely $\alpha = 1$ in $\chi_{eff}N = \phi_p^\alpha \chi_{AB}N$, are known to happen due to the reduction of intermolecular contacts that arises from the increase of the excluded-volume screening length upon solvent addition, leading to the theoretical prediction of $\alpha = 1.6$ in semi-dilute block copolymer solutions in nonselective good

solvents.⁴⁻⁶ This asymptotic value of the scaling exponent was confirmed even for concentrated regimes for nearly symmetric PS-b-PI copolymers in a neutral good solvent by Lodge et al.^{7,8} However, it is difficult to observe the asymptotic value of the exponent α in the simulation for small N .⁹ In order to estimate the exponent α in our model, we measure the number of intermolecular neighbors inside the range of the non-bonded interactions for a disordered system $\chi_{AB}N = 0$ in Figure S1. The number of intermolecular neighbors scales linearly to ϕ_p , confirming that the reduction of intermolecular contacts due to the increase of the excluded volume screening length upon solvent addition is negligible in our model, implying that α is close to unity in our model. Note that in our coarse-grained representation a bead corresponds to many monomeric repeat units in a chemically realistic model, and that our range of interaction (set by the bead size) is large compared to the typical range of atomistic interactions.

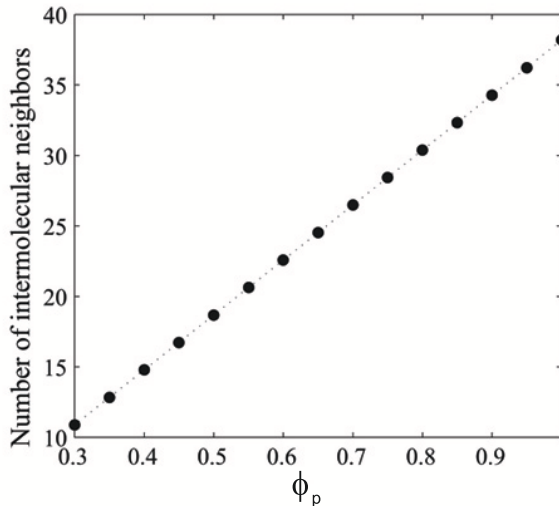


Figure S1: Number of beads that belong to a different polymers within the non-bonding interaction range (intermolecular contacts) as a function of polymer volume fraction ϕ_p ($N=32$)

Simulation methods

We conducted diffusive Monte Carlo calculations, which can capture the dynamics of collective densities that we are interested in, even if a MC scheme does not formally include hydrodynamics. This method has been used successfully to predict the phase separation kinetics of block copolymer thin films.^{10,11} Simulations are conducted in a rectangular simulation box with dimensions $L_x=3.46$, $L_y=6$ and $L_z=6$, in units of R_e , the average end-to-end distance of reference block copolymer chains in the melt. Periodic boundary conditions are used in the lateral (x and y) directions. In the normal (z) direction, on the bottom and top, we use impenetrable walls. The bottom wall represents the substrate and its interaction can be tuned depending on the experimental conditions of interest (e.g. chemically patterned substrate). $L_z=6$ is chosen to be well above the swollen film thickness; therefore the top wall is virtual, and does not interact with the block copolymer film and does not affect the film morphology; At each MC move, trial positions of polymer chains are generated for an individual bead or a group of beads using single-bead displacements or reptation moves. For solvent particles, only single bead displacements are performed. At each MC iteration step (MCS), each particle experiences one trial move on average. The probability of accepting the move is determined by the difference in total energy between the original and the trial configuration, and the weight factor as a function of polymer composition ϕ :²

$$P_{acc} = \frac{1}{(1 + \phi_o^8)^4(1 + \phi_n^8)^4} \min [1, \exp[-\Delta H/k_B T]] \quad (6)$$

where ϕ_o and ϕ_n are the polymer compositions at the original position r and the trial new location $r + \Delta r$. The weight function is defined to be less than unity, so it does not change the equilibrium distribution but suppresses the probability of accepting moves at high polymer concentration. The weight function captures the effect of varying mobility of the chain as a function of composition, such that systems with larger solvent volume fraction experience a larger probability of accepting a trial move. During a solvent annealing process, solvent

particles diffuse in and out of the polymer film, thus varying the polymer composition ϕ_p as a function of time. Moreover, depending on the relative speed between solvent particle diffusion through the film and solvent evaporation on the top of the film, ϕ_p can exhibit a gradient along the normal direction. Polymer composition becomes a time-dependent scalar field. The above mentioned rules reproduce the ϕ_p -dependent diffusivity, as shown in Figure S2. Diffusivity is measured from the mean-square displacement of bulk homopolymer solutions from simulations using the same rules for MC moves as in our block copolymer thin film simulations. There is a pronounced change in diffusivity for higher polymer concentration regions; for larger solvent volume fractions the diffusivity is nearly constant. This enables us to reproduce the fact that polymer chain mobility in the first region above T_g should vary rapidly, and it should level off as a function of solvent concentration. The profile we have chosen here can be tuned through the rules for proposing MC moves, and one can implement any realistic diffusivity provided by experiments.

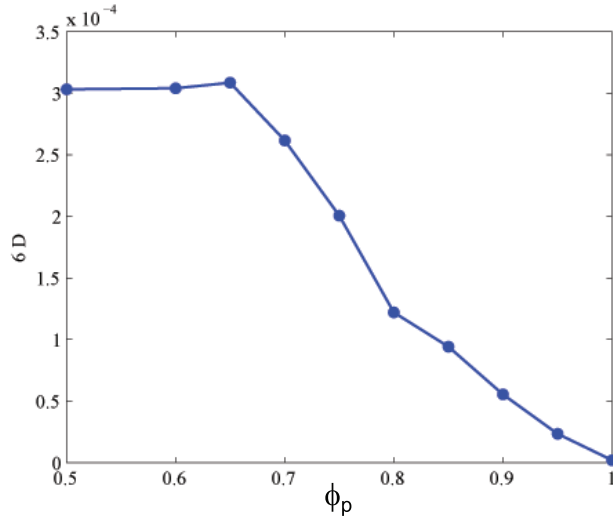


Figure S2: Diffusivity of polymer chains as a function of polymer volume fraction ϕ_p ($N=32$)

In order to evaluate the non-bonded energy, which is a functional of the local densities, a particle-to-mesh (PM) technique is employed. Local densities are defined from the positions of the beads.¹² In our model, solvent particles occupy a smaller volume than coarse-grained polymer beads. The radius of polymer beads is three times larger than that of solvent

particles when we chose $C_s = 30$ for PS and acetone. Thus the interaction range of solvent particles is smaller than that of polymer beads. A coarse-grained polymer bead corresponds to multiple monomeric repeating units and a solvent bead also corresponds to multiple acetone molecules. However, large $C_s = 30$ (thus the number of acetone molecules lumped into a solvent bead is smaller than that in a polymer bead) is chosen to keep the entropic contribution to the pressure (first order in particle number density) large enough to reproduce the solvent vapor phase under a wide range of pressures. We mapped beads onto a grid density using PM0 (the zeroth-order scheme where a bead is assigned to the nearest grid site with the entire weight) for the solvent, and using PM1 (the first-order scheme where a bead contributes to its eight neighboring sites, with linearly varying weights dictated by the distance between a grid site and a bead position) for polymer beads; solvent particles therefore have half the interaction range than polymer beads. Since 30 solvent particles occupy the volume of one polymer bead, computations with large numbers of solvent particles represent the most computationally demanding step in our model. An advantage of using a different PM scheme for polymer and solvent is that the computational load for solvent particles is reduced considerably by the simpler PM0 scheme. Throughout the simulations, we used a grid cell size to be $0.16 R_e$. Following past work, we also randomly displace the grid cell every 10 MC iterations in order to remove discretization artifacts introduced by the grid approach.¹²

References

- (1) Müller, M. *Phys. Rev. E* **2002**, *65*, 030802.
- (2) Müller, M.; Smith, G. D. *J. Polym. Sci. Part B: Polym. Phys.* **2005**, *43*, 934–958.
- (3) Hömberg, M.; Müller, M. *J. Chem. Phys.* **2010**, *132*, 155104–155104–18.
- (4) Olvera de la Cruz, M. *J. Chem. Phys.* **1989**, *90*, 1995–2002.
- (5) Fredrickson, G. H.; Leibler, L. *Macromolecules* **1989**, *22*, 1238–1250.

- (6) Guenza, M.; Schweizer, K. S. *Macromolecules* **1997**, *30*, 4205–4219.
- (7) Lodge, T. P.; Pan, C.; Jin, X.; Liu, Z.; Zhao, J.; Maurer, W. W.; Bates, F. S. *J. Polym. Sci. Part B: Polym. Phys.* **1995**, *33*, 2289–2293.
- (8) Lodge, T. P.; Hanley, K. J.; Pudil, B.; Alahapperuma, V. *Macromolecules* **2003**, *36*, 816–822.
- (9) Müller, M.; Binder, K.; Schäfer, L. *Macromolecules* **2000**, *33*, 4568–4580.
- (10) Detcheverry, F. A.; Nealey, P. F.; de Pablo, J. J. *Macromolecules* **2010**, *43*, 6495–6504.
- (11) Detcheverry, F. A.; Liu, G.; Nealey, P. F.; de Pablo, J. J. *Macromolecules* **2010**, *43*, 3446–3454.
- (12) Detcheverry, F. A.; Kang, H.; Daoulas, K. C.; Müller, M.; Nealey, P. F.; de Pablo, J. J. *Macromolecules* **2008**, *41*, 4989–5001.